scientific reports

Check for updates

OPEN

Modal analysis and frequency matching study of subway bogie frame under ambient excitation

Longjiang Shen✉ & Shizhong He

A wealth of practical cases indicates that the fatigue failure of subway bogies primarily stems from the modal resonance of the structure. If the modal characteristics of the entire vehicle, including equipment and bogies, are mismatched, rail vehicles may experience abnormal vibrations and noise. Therefore, it is imperative to conduct modal analysis and matching design for subway vehicle bogies to ensure smooth operation, reduce structural vibrations and noise, and enhance vehicle safety and ride comfort. Modal identification methods under the ambient l excitations during vehicle operation were employed to identify the modal parameters of the bogie structure before and after wheel reprofiling and under different load conditions. According to the test results, wheel reprofiling has minimal impact on the modal parameters of the structure, but with an increase in load, the modal frequencies of each order generally increase. This is associated with boundary constraint states, such as the increased stiffness of the bogie air spring with an increase in vehicle load. By comparing the test results with simulation analysis results of the bogie structure under free and constrained states, it is evident that simulating realistic boundary constraint conditions is crucial to ensure the accuracy of the finite element model. Based on frequency isolation criteria and vibration isolation theory, a frequency planning basis for the bogie structure was established. The study found that as the vehicle load increases, changes in the boundary conditions of the bogie affecting the elastic modal frequencies of the structure may have a certain impact on matching design, and may even better comply with the requirements of frequency management equations. This provides a new direction for subsequent scholars researching modal matching design.

Keywords Subway bogie, Modal experiment, Finite element analysis, Modal matching

Trains encounter diverse vibration environments with distinct characteristics during operation, such as periodic, random, and transient excitations, as well as combinations thereof. These different excitation types have varying impacts on equipment, potentially leading to resonance amplification, frequency coupling, functional failures, fatigue damage, and strength degradation. To mitigate these effects, it is critical to enhance the train's adaptability to vibration environments by avoiding resonance or significant amplification.

The bogie, a key component ensuring the safety and operational quality of the vehicle, supports, guides, and facilitates traction and braking[1]. Common issues include cracks at motor mount connections, antenna beam fractures, and axle box suspension ear breaks[2]. Modal resonance is often the root cause of fatigue failures in subway bogies. Misalignment of the modal characteristics of the entire vehicle, including its equipment and bogies, can lead to abnormal vibrations and noise[3].

Conducting modal analysis and matching design for subway vehicle bogies is essential to ensure smooth operation, reduce structural vibrations and noise, and enhance safety and ride comfort. Accurately determining the structural dynamics characteristics of rail vehicles is crucial for improving their dynamic performance. Structural modal parameters—modal frequencies, damping ratios, and mode shapes—are fundamental expressions of structural dynamics properties and are closely monitored during the design phase of rail vehicles.

Finite element numerical simulation[4] and vibration testing are the primary technical approaches currently used to obtain the structural modal parameters of rail vehicles. Test modal analysis is the process of modal identification of a research object under laboratory conditions or operational working conditions. Based on whether the external excitation signal is measurable during the identification process, test modal analysis methods can be classified into two categories[5]. Firstly, Experimental Modal Analysis (EMA), where the input signal of the system is controllable and measurable. The input excitation signal to the system is controllable and measurable. It involves analyzing and processing the response and excitation data to obtain the frequency

CRRC Zhuzhou Locomotive CO., LTD, Zhuzhou 412001, China. ✉email: 184272442@qq.com

response function of the structure. By combining modal identification methods, the inherent frequency, mode shapes, modal damping ratio, and other dynamic characteristic parameters of the structure can be identified. Secondly, Operational Modal Analysis (OMA), where the input signal of the system is not measurable, and the excitation signal comes from ambient excitations, with only the output response being measurable. OMA does not require measuring the input signal to the system. It solely relies on the output response under ambient excitation. Instead of frequency response functions, OMA replaces them with cross-correlation functions. By applying modal identification methods, the modal parameters of the structure can be identified. Compared to EMA, OMA can perform online analysis using only measured response signals, requires simpler equipment, and can identify modes that are easily excited under operational conditions.

Modal parameter identification methods in OMA can be classified according to various criteria. When categorized by the domain of identification, these methods are divided into frequency-domain and time-domain approaches. Frequency-domain methods, with their clear physical concepts and ease of representation of system responses in terms of amplitude and phase, were predominantly used in early identification techniques, such as peak picking[6] and circle fitting[6]. These techniques later evolved into more advanced methods like PolyMAX[7], which utilize common denominator models and matrix fraction descriptions.

Time-domain methods include the Ibrahim time-domain method[8,9], multiple reference point least-squares complex exponential method[10], and state-space model-based stochastic subspace methods[11,12] as well as time series methods[13,14]. More recently, blind source separation-based techniques have also been developed. A key advantage of time-domain methods is that they do not require transforming the measured time-domain signals into the frequency domain, thus avoiding potential errors associated with signal transformations.

Traditional frequency-domain identification methods typically rely on frequency response function information, or spectral matrices when input information is unavailable, and their accuracy is limited by data transformations between domains. Time-domain identification methods generally use impulse response functions and input–output time histories, substituting covariance and output time histories when input information is lacking, but they face challenges in selecting the correct model order. Methods for time-invariant structures in both time and frequency domains are well-established, while time–frequency domain methods that utilize time–frequency representations are more suitable for time-varying structures.

Due to limitations in traditional identification methods, there has been an emergence of intelligent identification methods based on smart algorithms. Regarding the identification model, methods can be categorized as non-parametric or parametric, and concerning the use of identification data, they can be batch or recursive. In terms of cost functions, methods include maximum likelihood, ridge regression, Kalman filtering, and Bayesian estimation. The three main elements—data, model set, and criterion or cost function—have undergone significant development: from single-output to multi-output data, from synchronous to asynchronous sampling; from non-parametric to parametric models, from single-channel to multi-channel models, and from frequency-domain to time-domain models; and from point estimation (such as least squares, maximum likelihood, ridge regression, Kalman filtering) to Bayesian estimation.

In railway vehicles, instability is related to modal shapes, and modal shapes have a damping rate that decreases as the driving speed increases. When the speed exceeds a certain value, the excitation from the track cannot be suppressed by the vehicle, resulting in an unstable state[15]. This unstable state leads to higher levels of acceleration experienced by passengers and higher interaction forces between the wheels and the track, which may pose safety hazards. Calvo et al.[16] used OMA to identify the vibration modes that cause vehicle instability. By applying OMA techniques to railway vehicles, a valuable application of OMA technology is proposed, which is to identify modal shapes corresponding to instability. Gong et al.[17] used the OMA method to identify the diamond deformation mode of the railway vehicle car body. They explained that the cause of the car body chattering is due to the coupled interaction between the car body diamond deformation mode and the hunting motion of the bogie. An optimization scheme for suspension parameters and wheel tread profiling was proposed, which significantly reduced the occurrence probability of car body chattering. Li et al.[18] compared simulation results with experimental results, suggesting that when conducting finite element analysis of the bogie structure's modal properties, it is essential to fully consider the constraints of the corresponding boundary conditions under operating conditions. There were significant differences between the tested structure and the free modal calculation results of the bogie structure during operation. Liu et al.[19] conducted modal testing on an operational high-speed train to obtain cross-spectral signals between structural response points and identify modal parameters. The modal parameter identification method used the least squares complex frequency domain method to obtain the actual modal parameters of the structure, which were then validated in conjunction with the measured vibration spectra of the axle boxes and the exterior floor of the car body.

However, there is currently no research on OMA of bogies under different vehicle loading states and different wheel wear conditions. There is a lack of studies and methodologies regarding modal matching of bogies and their attached components. Issues such as cracking and fatigue in bogie frames still occur frequently. Therefore, this paper adopts an operational modal parameter identification method based on ambient excitation to identify the modal parameters of the bogie frame. It conducts, for the first time, modal identification studies under different vehicle loading states (the tare loading (AW0) and the crush loading (AW3)) and different vehicle wear conditions, and compares these results with finite element simulations. The paper also compares modal calculation results considering the constraints of the bogie suspension and the influence of major components such as motors and gearboxes. Finally, based on a combination of frequency isolation criteria and vibration isolation theory, it proposes a frequency planning method for the bogie structure. Additionally, the modal matching design of the bogie under different conditions of wheel non-roundness is explored.

Operational modal identification methods

In this study, the PolyMax algorithm is used for operational modal identification of the steering frame. The PolyMax method is an extension of the multiple-reference least squares complex frequency domain method. It approximates the power spectral density of the output response instead of the frequency response function and minimizes the error using maximum likelihood estimation. This method allows for the identification of global modes, produces clearer steady-state diagrams, exhibits good anti-interference capabilities, and provides relatively high accuracy in parameter identification. For multiple output channel signals of the system, when selecting one channel as the reference point, the mathematical model of the cross-correlation function between each channel and the reference channel is expressed as follows[20]:

$$R_{m,1}(\tau) = \frac{1}{N}\sum_{k=0}^{N-1} y_m(k+\tau)y_1^T(k) \tag{1}$$

In the equation, k represents the numerical index of the test signal; y_1 represents the selected reference point; m represents the measurement point number; N represents the data length for each channel; τ represents the time delay; $R_{m,1}(\tau)$ represents the cross-correlation function between signals $y_1(k)$ and $y_m(k+\tau)$. Equation (1) is transformed into a power spectral density function through fast Fourier transform. Then, combined with the PolyMax algorithm, Eq. (2) is solved.

$$\mathbf{H}(\omega) = \mathbf{M}(\omega)\mathbf{N}(\omega)^{-1} \tag{2}$$

In this case, $\mathbf{H}(\omega)$ represents the frequency response function replaced by the power spectral density function, $\mathbf{M}(\omega)$ represents the numerator matrix polynomial, and $\mathbf{N}(\omega)$ represents the denominator matrix polynomial. The two matrices on the right side of Eq. (2) can be defined as follows:

$$\mathbf{M}(\omega) = \sum_{r=0}^{p} \mathbf{Z}^r \boldsymbol{\beta}_r \tag{3}$$

$$\mathbf{N}(\omega) = \sum_{r=0}^{p} \mathbf{Z}^r \boldsymbol{\alpha}_r \tag{4}$$

If the system has m-dimensional inputs and l-dimensional outputs, $\boldsymbol{\beta}_{r(l\times m)}$ represents the coefficient matrix polynomial for the numerator, and $\boldsymbol{\alpha}_{r(m\times m)}$ (r = 0, 1, …, p) represents the coefficient matrix polynomial for the denominator. Here, p is the chosen order of the mathematical model, Z represents the polynomial basis function $e^{-j\omega\Delta t}$, and Δt represents the sampling time. After selecting different frequencies, the coefficient matrix $[\boldsymbol{\beta}_r, \boldsymbol{\alpha}_r]$ can be approximated using the least squares method[21]. Based on the obtained coefficient matrix $\boldsymbol{\alpha}_r$ for the denominator, an extended unitary matrix is constructed, and then the unitary matrix is decomposed to obtain eigenvalues, which ultimately provides the modal participation factors and poles of the system. The modal participation factor matrix is located at the bottom row of the eigenvector matrix, and there exists the following relationship between the system poles p_i, p_i^* and the diagonal elements $\lambda_i, \lambda_i^* (i = 1, \ldots mp)$.

$$\lambda_i = e^{-p_i\Delta t}, \lambda_i^* = e^{-p_i^*\Delta t} \tag{5}$$

$$p_i, p_i^* = -\sigma_i \pm j\omega_{di} \tag{6}$$

The calculation Equation for modal damping ratio is:

$$\xi_i = \frac{\sigma_i}{\omega_i} = \frac{\sigma_i}{\sqrt{\sigma_i^2 + \omega_{di}^2}} \tag{7}$$

In the equation, ω_i represents the undamped natural frequency, and ω_{di} represents the damped natural frequency. After obtaining the poles p_i and modal participation factors $\mathbf{L}_i$, theoretically, all coefficients $\boldsymbol{\alpha}_r, \boldsymbol{\beta}_r$ can be calculated, and then substituted into Eq. (2) to obtain the modal shapes, as shown in the following equation:

$$\mathbf{H}(\omega) = \sum_{i=1}^{N}\left[\frac{\boldsymbol{\Phi}_i\mathbf{L}_i^T}{j\omega - p_i} + \frac{\boldsymbol{\Phi}_i\mathbf{L}_i^H}{j\omega - p_i^*}\right] - \frac{\mathbf{LR}}{\omega^2} + \mathbf{UR} \tag{8}$$

In the equation, $\boldsymbol{\Phi}_i$ represents the modal shape, $\mathbf{L}_i^T$ represents the modal participation factor row vector, $\mathbf{L}_i^H$ represents the conjugate transpose of $\mathbf{L}_i$, **LR** represents the low-frequency residue, and **UR** represents the high-frequency residue. Since the poles p_i and modal participation factors $\mathbf{L}_i$ have already been calculated, Eq. (8) can be formulated using the measured values of $\mathbf{H}(\omega)$ at different sampling frequencies. The unknown modal shapes $\boldsymbol{\Phi}_i$ as well as the low-frequency **LR** and high-frequency **UR** residues can be obtained using the linear least squares method.

Bogie modal test

The running modal experiments on the bogie frame of the subway vehicle were conducted under four different operating conditions, including the AW0 condition before reprofiling wheels, the AW3 condition before reprofiling wheels, the AW0 condition after reprofiling wheels, and the AW3 condition after reprofiling wheels. The identified running modal results of the bogie frame under different operating conditions were analyzed, and the subsequent finite element modal calculation results were validated and compared.

Testing protocol

Accelerometers were arranged on both sides of the subway bogie frame, with six sensors on each side on the side beams. Additionally, two acceleration sensors were placed on the crossbeam, one located at the midpoint and the other at the connection point between the motor and the crossbeam. Each motor on both sides was equipped with one acceleration sensor. There are 18 accelerometers in total. The vibration measurement points are shown in Fig. 1, The vibration measurement points are shown in Fig. 1, and the actual test point layout for the bogie frame is illustrated in Fig. 2. The selected accelerometers have a measurement range of ± 50 g. During the testing process, all acceleration sensors are configured to collect data synchronously, measuring both vertical and lateral vibration accelerations, with a sampling frequency set at 1024 Hz. A segment of stationary test signal is taken for modal identification, and the resulting modal parameters are used to validate subsequent finite element models.

In addition, the main experimental instruments and equipment used in the test, including data acquisition devices and handheld accelerometer calibrators, are shown in the Table 1.

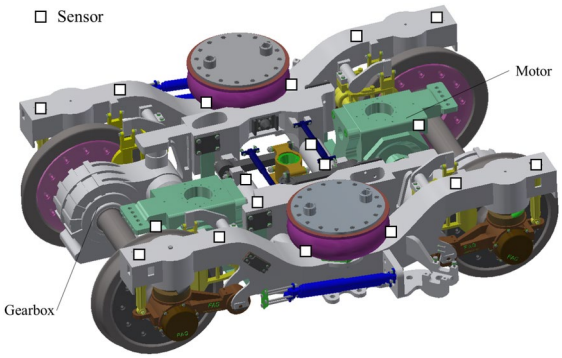

Fig. 1. Schematic diagram of the measurement points for the bogie frame vibration test.

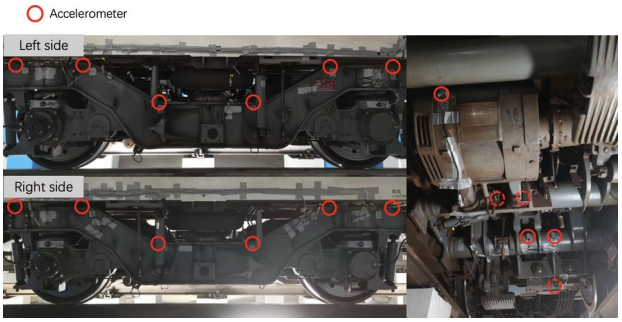

Fig. 2. Actual test point layout for the bogie frame.

Number	Instrument name	Quantity	Model	Producer
1	Three-axis accelerometer	18	–	Langs
2	Data acquisition system and analysis software	1	–	Oriental Institute
3	Portable accelerometer calibration instrument	2	JX-2A	Jinyang Wanda
4	Computer	1	ThinkPad	Lenovo

Table 1. Main experimental instruments.

Test results

In the same line section, modal testing is conducted on the bogie frame under different operating conditions. The tested conditions include four scenarios: AW0 reprofiled wheels before, AW0 reprofiled wheels after, AW3 reprofiled wheels before, AW3 reprofiled wheels after. Taking a certain measuring point at the end of the bogie frame as an example, the vertical and lateral vibration spectra under different testing conditions are shown in Fig. 3. It can be observed from Fig. 3 that regardless of the testing condition, as long as there is unevenness in the track, it can effectively stimulate the operational modes of the frame.

Based on the Polymax method, modal identification is performed using test data with a sample length of 30 s under constant speed operating conditions. Taking the AW0 reprofiled wheels before test condition as an example, the identified modal shapes of the bogie frame are shown in Fig. 4, and the modal frequency test results are shown in Table 2.

According to the statistical table of working modes for the bogie frame under different test conditions, it can be observed that for the bogie frame of the EMU bogie, the modal frequencies corresponding to the four modal mode shapes do not differ significantly between not reprofiled and reprofiled wheel conditions, with variations within ± 2%. Under different load conditions, the modal frequencies corresponding to the AW3 condition of the bogie frame are generally higher than those under the AW0 condition, which is related to the increase in load affecting the stiffness of the bogie frame air spring and other boundary constraint states.

Bogie frame structural modal analysis in simulation

Finite Element Modal Analysis is a structural vibration analysis method based on finite element calculations. It investigates the vibration characteristics of structures, including natural frequencies, mode shapes, and modal damping ratios, by discretizing the structure and employing principles and techniques of the finite element method.

Generally, the process of finite element modal analysis includes the following steps: Firstly, establish the geometric model of the object under study. Then, sequentially set the material properties, define contact relationships, perform meshing, and apply boundary conditions. Finally, conduct simulation analysis and output the simulation results. Therefore, based on the geometric model of the subway bogie frame, finite element modal analysis is performed, considering different constraint conditions, to calculate the modal results under different constraint states.

The software used for this modal analysis is Hypermesh. This software provides three main methods for extracting eigenvalues: the Power Method, the Transformation Method, and the Lanczos Method. Among these methods, the Lanczos Method combines the advantages of the previous two methods. It performs well and is

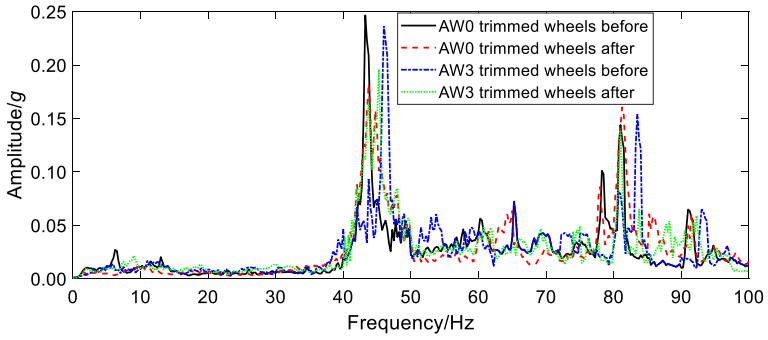

(a)

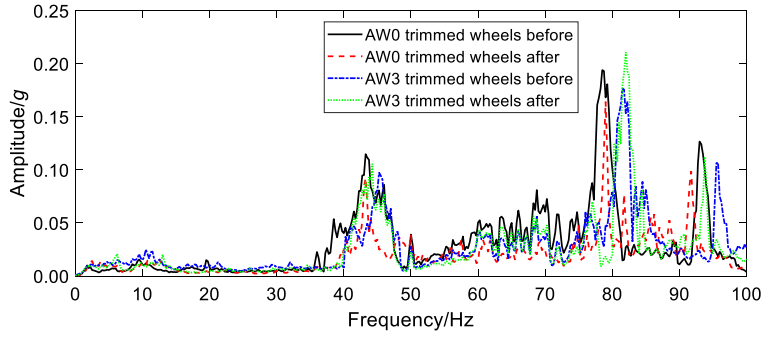

(b)

Fig. 3. Vibration spectrum of the measurement point at the end of the bogie frame under different test conditions.

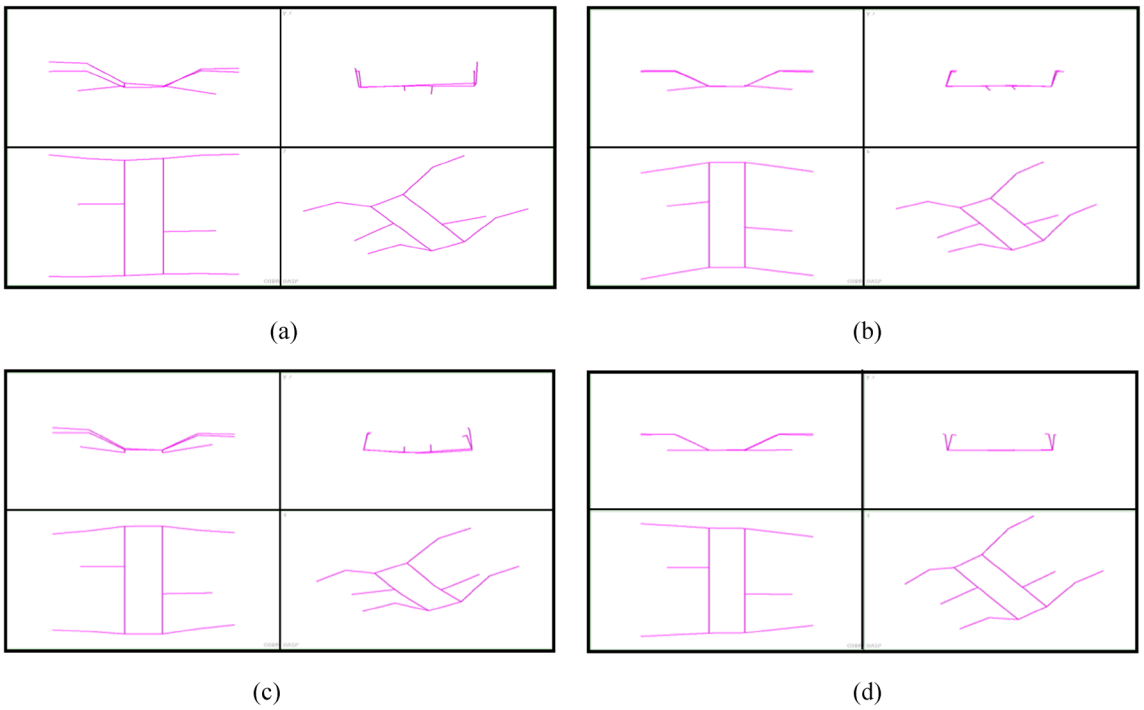

Fig. 4. Modal shapes of the bogie frame under different conditions.

Modal shape description	AW0 reprofiled wheels before/Hz	AW0 reprofiled wheels after/Hz	AW3 reprofiled wheels before/Hz	AW3 reprofiled wheels after/Hz
The frame torsion	43.829	44.369	46.158	45.257
The frame side beams is bent laterally	79.269	79.781	81.124	82.017
The frame cross beam is bent vertically	80.579	82.014	83.157	81.278
The horizontal plane of the frame side beam is deformed	93.667	92.357	95.458	94.285

Table 2. Statistical table of working modes for the bogie frame under different test conditions.

commonly used as the default method in most finite element software for calculating eigenvalues efficiently, without losing accuracy like the Transformation Method or the computational cost of the Power Method. Finite Element Modal Analysis is a structural vibration analysis method based on the finite element method. By discretizing the structure and combining the principles and techniques of the finite element method, it investigates the inherent characteristics of structural vibration, such as natural frequencies, mode shapes, modal mass, modal stiffness, and modal damping.

Establishment of finite element model

For the modal analysis of complex and large assemblies, it is reasonable to consider simplifying the geometric model to improve computational efficiency while ensuring accurate simulation analysis of the structure. Therefore, for complex large assemblies like the subway bogie frame, which consists of side beams, cross beams, and various welded structures such as motor mounts and brake hangers, the following simplifications can be applied:

(1) Ignore the auxiliary components of the frame, such as bolts and nuts.
(2) Neglect small fillets, chamfers, and other structural details.
(3) Disregard non-load-bearing structures, small-hole structures, and other insignificant small-sized structures.

These small structures not only increase the difficulty of meshing but also affect mesh quality, and they increase the computational workload by increasing the number of elements. Therefore, it is reasonable to consider their removal for simplification.

The main structural components of the bogie frame, such as side beams and cross beams, are connected by seamless welding and are primarily manufactured using carbon steel Q345E, as shown in Table 3, indicating its material properties.

Material	Density/(kg/m^3)	Elastic modulus /MPa	Poisson's ratio
Q345E	7850	2.1e5	0.3

Table 3. Material properties of the bogie frame.

Considering that the bogie frame is a complex and large assembly with irregular and diverse shapes, using a general automatic meshing method may not guarantee the quality of the mesh, leading to significant deviations between simulated modal results and actual conditions. Therefore, a manual meshing approach is employed to partition the bogie frame. To ensure mesh quality, suitable methods and sizes are chosen based on the actual dimensions of each component. Hexahedral elements are given priority for solid element meshing. Sweeping methods are applied for regular and simple structures, and mid-surface extraction combined with shell element meshing is employed for beam structures with length and width dimensions significantly larger than thickness. For assemblies consisting of multiple regular bodies, a multi-zone approach combined with tetrahedral meshing is utilized. Following these meshing methods, the overall model of the bogie frame is discretized into 312,793 elements with 668,101 nodes. Figure 5 illustrates the completed meshing of the bogie frame finite element model.

Modal simulation analysis

The bogie frame experiences constraints from the vehicle body, motor, gearbox, primary suspension, and secondary suspension during actual operation of the subway vehicle. The actual operational modes may differ from the results of free modal calculations. To obtain more accurate modal simulation results, it is essential to establish the boundary constraint conditions for the bogie frame.

Regarding the primary suspension, the actual constraint conditions are simulated by employing a series of parallel spring elements at the corresponding positions. These spring elements are connected to the frame at one end, and the other end is subjected to displacement constraints. The stiffness parameters of the spring elements match the actual design values.

For the secondary suspension, only the actual constraint conditions of the secondary series air springs are simulated. Spring elements are used at the positions of the secondary series air spring supports to simulate the actual constraint conditions during the operation of the frame. Similar to the primary suspension, one end of the spring element is connected to the frame, and the other end is subjected to displacement constraints. The stiffness parameters of the spring elements match the actual design values. Additionally, the vertical load forces applied by the vehicle body to the frame at this position are considered.

Regarding the constraints of the auxiliary equipment on the bogie frame, only the constraints of the heavier components, such as the motor and gearbox, are considered. The motor is simplified to a centroid structure using mass elements to approximate the actual structure, and spring elements are used to connect the motor mass element to the frame motor support. A relatively large stiffness value is set to simulate the rigid connection between the motor and the frame. Similarly, a centroid-simplified approach is used to simulate the gearbox's constraints, with spring elements representing the rigid connection between the gearbox and the frame.

Following the above boundary constraint method, the modal simulation calculation frequencies for the bogie frame under constrained conditions are shown in the Table 4, and the corresponding modal shapes are depicted in the Fig. 6. In order to investigate the influence of frame constraint conditions on the modal calculation results in the finite element model, a free modal calculation was performed on the frame, and the results are shown in Table 4.

Comparison of test results and finite element results

The final identification results of operational modes for the frame under different operating conditions and the finite element simulation modal calculation results under various constraint conditions are presented in Table 5.

Based on the test results, the simulated results under constrained ready-to-operate conditions for the dynamic car bogie frame are close to the test results under different loading conditions and wheelset conditions. The

Fig. 5. Finite element model of the bogie frame.

Modal order	Modal frequency in the load state /Hz	Modal frequency in the free state /Hz	Modal shape description
1	48.98	36.92	The frame torsion
2	82.80	64.44	The side beams lateral bending mode
3	84.17	64.97	The side beams vertical bending mode
4	102.57	76.69	The side beam horizontal bending mode

Table 4. Modal frequencies of the bogie frame under readiness and free-state.

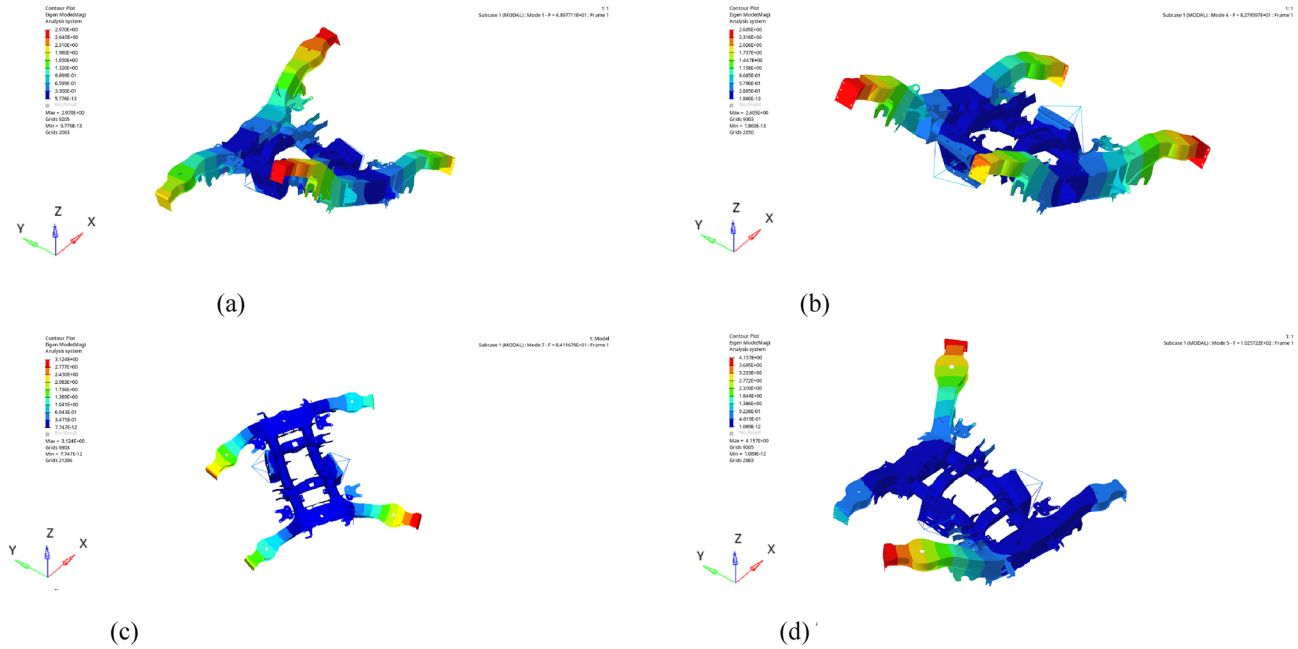

Fig. 6. Modal shape diagram of bogie frame.

Modal shape description	AW0 reprofiled wheels before	AW0 reprofiled wheels after	AW3 reprofiled wheels before	AW3 reprofiled wheels after	Modal frequency in the free state	Modal frequency in the load state
The frame torsion	43.829	44.369	46.158	45.257	36.92	48.98
The side beams lateral bending mode	79.269	79.781	81.124	82.017	64.44	84.17
The side beams vertical bending mode	80.579	82.014	83.157	81.278	64.97	82.80
The side beam horizontal bending mode	93.667	92.357	95.458	94.285	76.69	102.57

Table 5. Statistical table of modal parameters for different operating conditions: test results versus finite element simulation results.

deviation is around 10%, with a maximum deviation of 13% and an average deviation of 6.7%. However, under the free state, the results show larger deviations from the test results under different conditions, with deviations around 20%, a maximum deviation of 28%, and an average deviation of 23.7%. This indicates that there is a significant difference in the finite element modal calculation results under different constraint conditions. It is essential to simulate the actual boundary conditions as closely as possible to ensure the accuracy of the finite element model.

Modal frequency matching of bogie frame

Structural vibration is a superposition of modes. To prevent resonance and reduce amplification factors, it is necessary to consider the frequency matching relationships between excitation sources, the entire system, subsystems, and substructures. Through frequency planning, combined with finite element simulation and on-site testing, it is possible to comprehensively analyze the excitation frequencies of the bogie and their hierarchical

frequencies. This helps to clarify the frequency isolation status of the bogie and its major mass components, providing a reference for structural optimization design. In this analysis, the bogie frame is taken as an example to analyze the matching design between the bogie and wheel polygons, and the impact of different loading conditions on matching design is discussed.

Main structure and known forced excitation relationship

Based on frequency isolation criteria

According to vibration theory calculations, it is understood that severe vibrations will occur in a system at its resonance frequency. However, in practical systems, intense vibrations occur not only precisely at the resonance frequency. When the excitation frequency falls within a region near the calculated resonance frequency, the system will undergo resonance. This region is referred to as the resonance region. The range of the resonance region is typically determined using the half-power bandwidth. This is illustrated by the vibrational response of a single-degree-of-freedom system, as shown in Fig. 7. The system's vibration transmissibility $T(f)$ reaches its maximum at frequency $f = f_n$, with an amplification factor $Q = 1/(2\zeta)$.

From Fig. 7, it can be observed that regardless of how damping varies, when the natural frequency f_n of the system is at a certain distance from the excitation frequency f, the system's vibrational response rapidly decreases. Therefore, for a single-degree-of-freedom system, the isolation criterion between the excitation frequency and the system frequency, based on the half-power bandwidth, can be formulated as:

$$f < 0.7f_n \text{ or } f > 1.414f_n \tag{9}$$

For multi-degree-of-freedom systems, they can be transformed into a series of single-degree-of-freedom systems. In this analysis, the focus is primarily on the first 3–5 modes of each hierarchical system. Similarly, for multi-degree-of-freedom systems, the isolation criterion between the excitation frequency and the system frequency, based on the half-power bandwidth, can be formulated as:

$$f < 0.7f_1 \text{ or } 1.414f_n < f < 0.7f_{n+1}, n = 1, 2, \ldots \tag{10}$$

In the equation: f_1 is the first-order mode of the system; f_n and f_{n+1} are the natural frequencies of adjacent two-order system modes, and $f_n < f_{n+1}$.

For local structures with high natural frequencies exceeding 1000 Hz, and relatively low inherent damping, achieving the criterion in the above equation can be computationally expensive. Therefore, in this analysis, the isolation criterion between the excitation frequency and the system frequency for high-frequency local structures is:

$$f < 0.85f_1 \text{ or } 1.15f_n < f < 0.85f_{n+1}, \ n = 1, 2, \cdots \tag{11}$$

Based on vibration isolation theory

In terms of vibration transmission direction, isolation measures can be classified into two categories: active isolation and passive isolation. Active isolation aims to isolate the vibration source, meaning an object that is itself a source of vibration. To reduce its impact on surrounding equipment, it is isolated from the entire foundation. Passive isolation, on the other hand, aims to isolate the response. For instruments or devices that allow only small vibrations, and to prevent the influence of surrounding vibration sources, they are isolated from the entire foundation. For both types of isolation, the transmissibility can be expressed as:

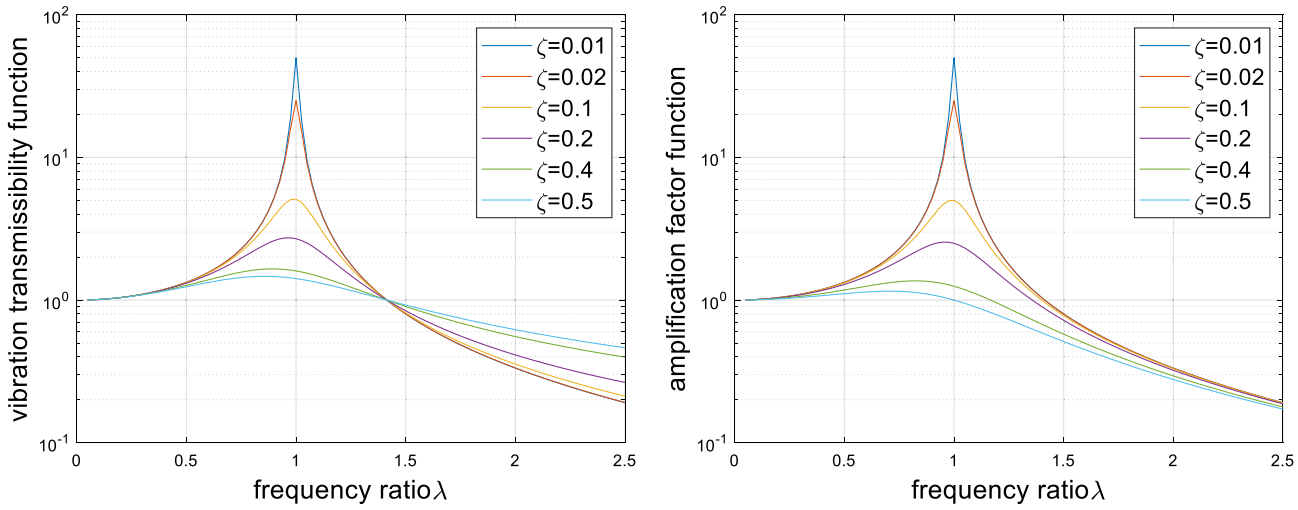

Fig. 7. Dynamic response curve.

$$\eta = \sqrt{\frac{1 + 4\zeta^2\lambda^2}{\left(1 - \lambda^2\right)^2 + 4\zeta^2\lambda^2}} \tag{12}$$

In the equation, λ is the ratio of the excitation frequency f to the modal frequency f_0, and ζ is the modal damping ratio.

Based on extensive engineering experience, the modal damping ratio for rail vehicle structures typically ranges from 0.1 to 5%. Figure 8 illustrates the transmissibility of existing rail vehicle structures with different damping ratios. The figure is divided into two regions. In the vicinity of point $\lambda = 1$, structures with different damping ratios exhibit pronounced resonance regions. However, as the frequency ratio λ surpasses a certain range, the damping ratio no longer affects the vibration transmissibility of rail vehicles. If the difference in transmissibility for different modal damping ratios is within 3%, their response to frequency ratio changes is relatively small, as shown in Fig. 8.

$$\eta_{0.1\%} - \eta_{5\%} > 3\%\eta_{5\%} \tag{13}$$

Substituting Eqs. (13) into (12), we obtain $0.82 < \lambda < 1.20$, representing a more effective isolation:

$$f < 0.82 f_0 \text{ or } f > 1.20 f_0 \tag{14}$$

At this stage, despite adjustments to the modal damping ratio, relatively high levels of transmissibility may still occur, indicating ineffective vibration isolation. Therefore, in engineering applications, it is advisable to avoid having the excitation frequency fall within this critical range.

Frequency management based on wheel polygons

With the continuous increase in train speed and running mileage, the operational boundary conditions of rail vehicles are constantly changing. During train operation, wheel-rail excitation and the resulting vibrational response still play a significant role. The wheel surface roughness (wheel polygons) is one of the main influencing factors of wheel-rail excitation. In this analysis, we mainly consider wheel polygons as the primary dynamic excitation load affecting the bogie.

In the process of wheel rolling along the steel rail, the excitation frequency generated by the *i*-th order polygon of the wheel can be calculated using Eq. (15).

$$f_i = \frac{v \times r_i}{3.6 \times \pi \times D} \tag{15}$$

In the equation, v represents the train speed in km/h, r_i is the wheel polygon order, and D is the semi-worn diameter of the wheel (0.84 m).

In this analysis, considering the design speed of the train is 120kmh, it is mainly concerned that the train traction motor is in the characteristic interval speed, that is, the train speed interval is 100kmh to 120kmh, and the motor output torque is low at this time, and the vehicle is used to running at a uniform speed under this speed level.

This analysis focuses on the modal frequencies of the bogie and its various components under different states of maintenance. The order characteristics of different wheels exhibits varying distributions. Typically, the order distribution for a well-maintained wheel is dominated by low-order components up to the third order. The histogram depicting the distribution of wheel roughness levels, from low to high order, closely follows the limit curve specified by ISO 3095. As the order increases, the roughness level decreases. This study primarily examines the impact of the first five orders of wheel polytonality. The frequency at which these orders occur at specific speeds is detailed in Table 6.

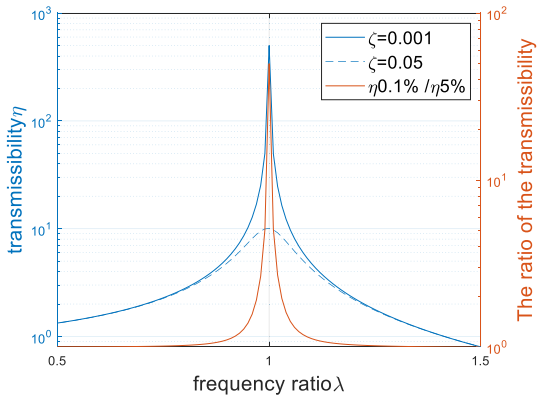

Fig. 8. Vibration transmissibility of rail vehicles.

Order	Vehicle speed/(km/h)		
	100 (Hz)	110 (Hz)	120 (Hz)
1	10.53	11.58	12.63
2	21.05	23.16	25.26
3	31.59	34.74	37.89
4	42.10	46.31	50.52
5	52.63	57.89	63.15

Table 6. Dynamic excitation of different wheel non-rounding orders at different vehicle speeds.

In this analysis, the frequency planning management object includes only the bogie frame structure. Based on the operational modal test results under the conditions of "Before Wheelset AW0" and "Before Wheelset AW3," it is observed that the main frequencies of the bogie frame are below 100 Hz. This allows the use of Eq. (11) as the basis for frequency planning.

Considering the dynamic excitation frequencies of wheel polygons at different train speeds, taking the train speed as 100 km/h as an example, the excitation frequencies for wheel polygons at the 3rd, 4th, and 5th orders are 31.59 Hz, 42.10 Hz, and 52.63 Hz, respectively. Under the "Before Wheelset AW0" condition, the first modal frequency of the bogie frame is 43.829 Hz. It does not satisfy Eq. (11) under the excitation of wheel polygons at the 4th and 5th orders. Under the excitation of wheel polygons at the 3rd order, it does not satisfy Eq. (13). In the "Before Wheelset AW3" condition, the first modal frequency of the bogie frame is 46.158 Hz. Under the excitation of wheel polygons at the 4th and 5th orders, it does not satisfy Eq. (11), without interference from the frequency of wheel polygons at the 3rd order.

Therefore, as the vehicle's load increases, the changes in the boundary conditions of the bogie affect the elastic modal frequencies of the frame. This may have an impact on modal matching design and could better satisfy frequency management Equations. This provides a new direction for further research by other scholars in modal matching design.

Conclusion

For the subway bogie frame, there is little difference in modal frequencies for frame torsion, lateral bending of the side beams, vertical bending of the frame cross beams, and deformation of the horizontal plane of the side beams between the conditions "before wheel reprofiling" and "after wheel reprofiling." Variations in these modal frequencies are within ± 2%, indicating that the wheelset has minimal impact on the modal characteristics of the bogie frame. Under different loading conditions, the modal frequencies corresponding to the "AW3 after wheel reprofiling" condition are generally higher than those for the "AW0 before wheel reprofiling" condition. This is attributed to the increased load affecting the stiffness of the bogie air springs and other boundary constraint states.

Under various loading and wheel reprofiling conditions, the simulated results of the bogie frame in the constrained state closely match the test results under different conditions, with discrepancies of approximately 10%, a maximum deviation of 13%, and an average deviation of 6.7%. However, in the free state, the simulation results deviate significantly from the test structures under different conditions, with discrepancies of around 20%, a maximum deviation of 28%, and an average deviation of 23.7%. This indicates that there are significant differences in finite element modal calculation results under different constraint conditions, and efforts should be made to simulate realistic boundary constraint states to ensure the accuracy of the finite element model.

Combining frequency isolation criteria and vibration isolation theory can provide a basis for the frequency planning of the bogie frame. When the vehicle load increases, changes in the boundary conditions of the bogie affect the elastic modal frequencies of the frame. This may have implications for modal matching design and could better satisfy frequency management Equations. This provides a new direction for further research by other scholars in modal matching design.

Despite providing useful insights into the modal characteristics of the bogie frame, there are several limitations that need to be acknowledged. Firstly, the load conditions used in the experiments (such as AW0 and AW3) are specific and may not fully represent the load distribution encountered in all vehicle load environments. Secondly, the discrepancies between the simulation results and the experimental results indicate that the current finite element model may not completely capture all the intricate details of the actual bogie frame. Additionally, while this study focuses on the conditions before and after wheelset reprofiling, it does not consider other factors that might influence the modal characteristics, such as wheel diameter differences.

Compared to relevant previous studies, the results of this study have a certain degree of generality, particularly regarding the relationship between modal frequencies and load changes. However, given the differences between different vehicle models and manufacturers, the direct application of the study's results may require adjustments based on specific circumstances. To enhance the general applicability of the research findings, future studies could consider a wider range of boundary conditions and more complex models to more accurately reflect real-world operating conditions.

Data availability

The data that support the findings of this study are available on request from the corresponding author upon reasonable request. Coinv DASP V11, http://www.coinv.com/node/id/50463232.html; MATLAB 2022b, https://ww2.mathworks.cn/; HyperWorks 2019X https://www.altair.com.cn/.

Received: 10 January 2024; Accepted: 4 September 2024
Published online: 14 September 2024

References

1. Jinsong, Z. *Vibration and Control of Railway Vehicles* (Fudan University Press, 2020).
2. Wei, L. *et al.* Hunting stability and dynamic stress analysis of a high-speed bogie using elastic-suspended motors as dynamic vibration absorber. *Veh. Syst. Dyn.* **62**(9), 2332–2354. https://doi.org/10.1080/00423114.2023.2289654 (2024).
3. Liu, G. *et al.* Research on resonance mechanism of articulated train car body based on modal vibration extraction method. *J. Vib. Control* https://doi.org/10.1177/10775463241256017 (2024).
4. Gong, D. *et al.* Frequency veering between car body and under-chassis equipment of railway vehicles in vertical bending mode. *Mech. Syst. Signal Process.* **185**, 109768 (2023).
5. Orlowitz, E. & Brandt, A. Comparison of experimental and operational modal analysis on a laboratory test plate. *Measurement* **102**, 121–130 (2017).
6. Heylen, W. *et al. Modal Analysis Theory and Testing* (Katholieke Universiteit Leuven, 1997).
7. Peeters, B. *et al.* The PolyMAX frequency-domain method: A new standard for modal parameter estimation. *Shock Vib.* **11**, 395–409 (2004).
8. Ibrahim, S. R. Random decrement technique for modal identification of structures. *J. Spacecr. Rockets* **14**(11), 696–700 (1977).
9. Ibrahim, S. R. & Pappa, R. S. Large modal survey testing using the Ibrahim time domain identification technique. *J. Spacecr. Rockets* **19**(5), 459–465 (1982).
10. Brown, D. L. *et al.* Parameter estimation techniques for modal analysis. *SAE Pap.* **88**(2), 299–305 (1979).
11. Overschee, P. V. & Moor, B. D. Subspace algorithms for the stochastic identification problem. *Automatica* **29**(3), 649–660 (1993).
12. Peeters, B. & Roeck, G. D. Stochastic system identification for operational modal analysis: A review. *J. Dyn. Syst. Meas. Control* **123**(4), 659–667 (2001).
13. Moore, S. M. *et al.* ARMAX modal parameter identification in the presence of unmeasured excitation I: Theoretical background. *Mech. Syst. Signal Process.* **21**(4), 1601–1615 (2007).
14. Moore, S. M. *et al.* ARMAX modal parameter identification in the presence of unmeasured excitation II: Numerical and experimental verification. *Mech. Syst. Signal Process.* **21**(4), 1616–1641 (2007).
15. Wang, Z. *et al.* A survey on countermeasures of railway vehicle stability decrease caused by the evolution of hollow-worn wheels. *J. Vib. Control* https://doi.org/10.1177/10775463241234726 (2024).
16. Calvo, L. E. *et al.* Analysis of instabilities in railway vehicles employing operational modal analysis. In *Joint Rail Conference American Society of Mechanical Engineers* https://doi.org/10.1115/JRC2015-5697 (2015).
17. Gong, D. *et al.* Research on mechanism and control methods of carbody chattering of an electric multiple-unit train. *Multibody Syst. Dyn.* **53**, 135–172 (2021).
18. Jian, L. *et al.* Operational modal analysis of bogie frame and its effect on vibration transfer of high-speed train. *Noise Vib. Control* **35**(3), 5 (2015).
19. Liu, G. *et al.* Frequency veering of railway vehicle systems and its mapping to vibration characteristics. *Multibody Syst. Dyn.* https://doi.org/10.1007/s11044-024-09989-x (2024).
20. Brandt, A. *Modal Analysis Theory* (Wiley, 2011).
21. Josué, P. & Oliver, P. Vibration-based damage detection in a wind turbine blade through operational modal analysis under wind excitation. *Mater. Today Proc.* **56**(1), 291–297 (2022).

Author contributions

Conceptualization, S.L. and H.S.; methodology, S.L.; software, H.S.; validation S.L. and H.S.; formal analysis, S.L.; investigation, H.S.; resources, S.L.; data curation, H.S.; writing—original draft preparation, H.S.; writing—review and editing, S.L.; visualization, H.S.; supervision, H.S.; project administration, S.L.; funding acquisition, H.S. All authors have read and agreed to the published version of the manuscript.

Funding

Original Technology 10-Year Cultivation Special Project of CRRC Corporation Limited (2022CYY007).

Competing interests

The authors declare no competing interests.

Additional information

Supplementary Information The online version contains supplementary material available at https://doi.org/10.1038/s41598-024-72146-z.

Correspondence and requests for materials should be addressed to L.S.